Securing Reconfigurable Holographic Surfaces Assisted 6G Wireless Systems

Chandan Kumar Sheemar, Wali Ullah Khan, and Symeon Chatzinotas, *Fellow, IEEE*
SnT, University of Luxembourg, Luxembourg
e-mails:{chandankumar.sheemar,waliullah.khan,symeon.chatzinotas}@uni.lu,

***Abstract*—This paper investigates the problem of secrecy rate maximization in reconfigurable holographic surface (RHS)-assisted systems by jointly designing digital and analog holographic beamformers. The problem is inherently non-convex and challenging to solve. To address this, we propose a novel alternating optimization algorithm based on the minorization-maximization (MM) framework, leveraging surrogate functions for efficient and reliable optimization. In the proposed approach, digital beamforming directs signal power toward the legitimate user while minimizing leakage to unintended receivers, and holographic beamforming refines wavefronts to further enhance secrecy performance. Simulation results validate the effectiveness of the proposed framework, showing significant secrecy rate improvements over benchmark methods.**

***Index Terms*—holographic beamforming, secrecy rate maximization, minorization-minimization**

I. Introduction

With the emergence of new applications envisioned in 6G, wireless systems are expected to handle increasingly sensitive data while operating in more dynamic and complex environments [1]. Recently, reconfigurable holographic surfaces (RHS) have emerged as a groundbreaking paradigm in wireless communications, offering unprecedented capabilities to enhance the performance and security of wireless systems [2]. An RHS is an array of programmable elements that can dynamically manipulate electromagnetic waves, enabling fine-grained control over the wireless propagation environment. By leveraging advanced materials and holographic principles, RHS can steer, focus, and scatter signals with high precision, adapting to varying channel conditions, user locations, and interference patterns. Unlike traditional antenna arrays, RHS is highly energy-efficient, operating with minimal power consumption while delivering exceptional control over wavefronts [**?**], [3], [4].

Recent research on RHS-assisted wireless systems has explored spatial characteristics, beamforming strategies, security, and joint communication-sensing capabilities. In [5], the spatial degrees of freedom (DoF) and ergodic capacity in point-to-point and LoS holographic communications are analyzed, while [6] proposes low-complexity RIS-aided designs with closed-form configurations. In [7], the authors investigate holographic joint communication and sensing (JCAS) under Cramer-Rao bounds, while [8] addresses joint holographic beamforming for 3D unmanned aerial vehicle (UAV) communications. Additionally, [9] explores hybrid holographic beamforming and user scheduling for sum-rate maximization under individual QoS constraints. In the realm of security, [10] examines secrecy rate maximization for single-RF-chain transceivers without RHS, resulting in energy-inefficient and costly solutions. The work in [11] attempts secrecy rate optimization with holographic beamforming using a traversal-based approach, which remains highly sub-optimal. These studies underscore the need for advanced algorithms that fully exploit RHS capabilities, paving the way for more sustainable and secure wireless ecosystem.

This work presents a novel framework for secrecy rate maximization in hybrid RHS-assisted systems by jointly optimizing digital beamforming and analog holographic beamforming. Unlike previous studies, we assume that we have multiple RF chains and optimize the holographic beamforming under practical amplitude constraints due to the RHS. We employ a minorization-minimization (MM)-based alternating optimization approach, enabling an efficient hybrid holographic beamforming design. The proposed method iteratively constructs convex surrogate functions to tackle the inherent non-convexity of the problem. First, closed-form expressions for the surrogate functions are derived and their validity is established. Then, an alternating optimization algorithm is developed, where the joint problem is decomposed into two sub-problems, each solved while keeping the other variable fixed. For holographic beamforming, the MM framework is integrated with the gradient ascent method to optimize the holographic weights while ensuring compliance with the amplitude box constraints. Simulation results validate the effectiveness of the proposed approach, demonstrating significant secrecy rate improvements over the benchmark method. Our findings position RHS-assisted systems, coupled with MM-based optimization, as a promising solution for secure wireless communications.

Notations: In this paper, we adopt a consistent set of notations: Scalars are denoted by lowercase or uppercase letters, while vectors and matrices are represented by bold lowercase and bold uppercase letters, respectively. The transpose, Hermitian transpose, and inverse of a matrix $\mathbf{X}$ are denoted by $\mathbf{X}^{\mathrm{T}}$, $\mathbf{X}^{\mathrm{H}}$, and $\mathbf{X}^{-1}$, respectively. Sets are indicated by calligraphic letters (e.g., $\mathcal{X}$), and their cardinality is represented by $|\mathcal{X}|$. Finally, $|\cdot|$ denotes the l_2-norm.

II. System Model

A. Scenario Description

We consider a downlink communication system that consists of one base station (BS) (referred to as Alice), one legitimate

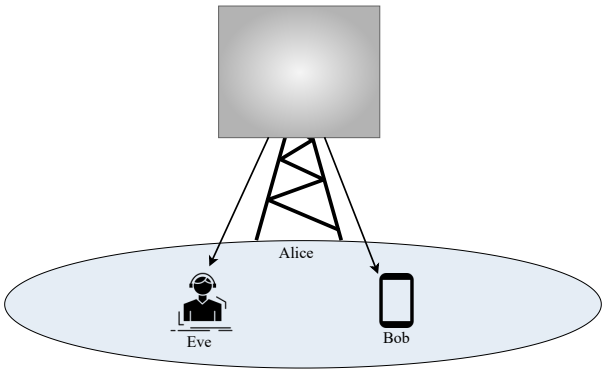

Fig. 1: RHS-assisted secure holographic communications.

user (referred to as Bob), and one intended recipient (referred to as Eve), as shown in Figure 1. The BS employs a hybrid beamforming architecture, which consists of two components: a high-dimensional holographic beamformer in the analog domain and a lower-dimensional digital beamforming. The BS is equipped with R RF chains and generates the digitally beamformed signal using the digital beamforming vector $\mathbf{v} \in \mathbb{C}^{R\times 1}$, optimized for Bob. We assume that each RF chain feeds its corresponding RHS feed, transforming the high-frequency electrical signal into a propagating electromagnetic wave. The digitally processed signal is further multiplied by the analog holographic beamforming matrix $\mathbf{W} \in \mathbb{C}^{M\times R}$, implemented by the RHS. The RHS consists of M reconfigurable elements arranged in a rectangular grid with $\sqrt{M}$ elements along each axis. Each element of the holographic beamforming matrix $\mathbf{W}$ is represented as $\{w_m \cdot e^{-j\mathbf{k}_s\cdot\mathbf{r}_m}\}$ [12], where w_m denotes the holographic weight of the radiation signal at the m-th element to enable holographic beamforming, and $e^{-j\mathbf{k}_s\cdot\mathbf{r}_m}$ represents the phase shift determined by the reference wave vector $\mathbf{k}_s$, and $\mathbf{r}_m$ denotes the position of the m-th element.

Let $s \sim \mathcal{CN}(\mathbf{0}, 1)$ denote the transmitted data stream to the intended user Bob. Given the aforementioned notations, the received signal at Bob can be written as

$$y_b = \mathbf{h}_b^H \mathbf{W}\mathbf{v}s + n_b, \tag{1}$$

where $\mathbf{h}_b \in \mathbb{C}^{M\times 1}$ is the channel vector between the Alice and Bob, and $n_b \sim \mathcal{CN}(0, \sigma_b^2)$ represents the additive white Gaussian noise (AWGN) at Bob. Similarly, the received signal at Eve can be expressed as

$$y_e = \mathbf{g}_e^H \mathbf{W}\mathbf{v}s + n_e, \tag{2}$$

where $\mathbf{g}_e \in \mathbb{C}^{M\times 1}$ is the channel vector between the Alice and Eve, and $n_e \sim \mathcal{CN}(0, \sigma^2)$ represents the AWGN at Eve.

B. Problem Formulation

The objective of this work is to maximize the secrecy rate of Bob, while ensuring that the information leakage to Eve is minimized. To define the secrecy rate, we first define the signal-to-interference-plus noise (SINR) both at Bob and Eve, given as

$$\text{SINR}_b = |\mathbf{h}_b^H \mathbf{W}\mathbf{v}|^2/\sigma_b^2, \quad \text{SINR}_e = |\mathbf{g}_b^H \mathbf{W}\mathbf{v}|^2/\sigma_e^2. \tag{3}$$

The secrecy rate maximization problem is then formulated as

$$\max_{\mathbf{v},\mathbf{W}} \Big[\log_2(1+\text{SINR}_b) - \log_2(1+\text{SINR}_e)\Big]^+, \tag{4a}$$

$$\text{s.t.} \quad \text{Tr}\left(\mathbf{W}\mathbf{v}\mathbf{v}^H\mathbf{W}^H\right) \le P_t, \tag{4b}$$

$$0 \le w_m \le 1, \quad \forall m \in \{1,\dots,M\}, \tag{4c}$$

where P_t is Alice's total transmit power budget. Constraint (4b) ensures the total power of the transmitted signal does not exceed the power budget, while constraint (4c) enforces the amplitude of the RHS elements [12].

III. MM-Based Secrecy Rate Maximization

To solve this challenging problem, we employ an alternating optimization approach integrated with the MM- MM-principle [13], to decompose the joint optimization problem into manageable subproblems.

A. Digital Beamforming Optimization via MM

We optimize the digital beamforming vector $\mathbf{v} \in \mathbb{C}^{R\times 1}$ while fixing the analog beamformer $\mathbf{W} \in \mathbb{C}^{M\times R}$. Let $\mathbf{Q}_b = \mathbf{W}^H\mathbf{h}_b\mathbf{h}_b^H\mathbf{W}$ and $\mathbf{Q}_e = \mathbf{W}^H\mathbf{g}_e\mathbf{g}_e^H\mathbf{W}$, and define the constants $c_b = \sigma_b^2$, $c_e = \sigma_e^2$. The secrecy rate becomes

$$R_s(\mathbf{v}) = \left[\log_2\left(1+\frac{\mathbf{v}^H\mathbf{Q}_b\mathbf{v}}{c_b}\right) - \log_2\left(1+\frac{\mathbf{v}^H\mathbf{Q}_e\mathbf{v}}{c_e}\right)\right]^+. \tag{5}$$

Since this is a difference of concave functions, we employ the MM framework to iteratively optimize a minorize surrogate function. We retain the first term in the surrogate exactly, as it is already concave in $\mathbf{v}$. For the second term, observe that the function $f(x) = \log_2(1+x)$ is concave for $x \ge 0$, but it appears with a minus sign, making it convex. The first-order Taylor expansion of a concave function at any point x_0 satisfies the following upper bound

$$f(x) \le f(x_0) + f'(x_0)(x - x_0), \tag{6}$$

which yields a global upper bound. Negating both sides of, we get to the following minorized objective function

$$\mathcal{L}_v^{(t)}(\mathbf{v}) = \log_2\left(1+\frac{\mathbf{v}^H\mathbf{Q}_b\mathbf{v}}{c_b}\right) - \frac{1}{\ln 2}\cdot\frac{\mathbf{v}^H\mathbf{Q}_e\mathbf{v}}{(1+\gamma_e^{(t)})c_e}, \tag{7}$$

where $\gamma_e^{(t)}$ is the SINR at Eve from the previous iteration. To enable closed-form optimization, we exploit the monotonicity of the log function and equivalently maximize the ratio argument:

$$\max_{\mathbf{v}} \mathbf{v}^H \underbrace{\left(\frac{\mathbf{Q}_b}{c_b} - \frac{1}{\ln 2}\cdot\frac{\mathbf{Q}_e}{(1+\gamma_e^{(t)})c_e}\right)}_{=\mathbf{Q}_v}\mathbf{v}, \quad \text{s.t. } \|\mathbf{W}\mathbf{v}\|^2 \le P_{\text{t}}. \tag{8}$$

Let us define the Lagrangian for the problem, given as

$$\mathcal{L}(\mathbf{v},\lambda) = \mathbf{v}^H\mathbf{Q}_v^{(t)}\mathbf{v} - \lambda\left(\mathbf{v}^H\mathbf{W}^H\mathbf{W}\mathbf{v} - P_{\text{av}}\right), \tag{9}$$

where $\lambda \geq 0$ is the Lagrange multiplier associated with the inequality constraint. To find the stationary points, we take the derivative of $\mathcal{L}$ with respect to $\mathbf{v}^H$ and set it to zero as follows

$$\frac{\partial \mathcal{L}}{\partial \mathbf{v}^H} = 2\mathbf{Q}_v^{(t)}\mathbf{v} - 2\lambda \mathbf{W}^H\mathbf{W}\mathbf{v} = \mathbf{0}. \tag{10}$$

Dividing both sides by 2 and rearranging terms, we obtain the generalized eigenvalue equation [14], [15]

$$\mathbf{Q}_v^{(t)}\mathbf{v} = \lambda \mathbf{W}^H\mathbf{W}\mathbf{v}. \tag{11}$$

This equation is exactly the definition of a generalized eigenvalue problem for the matrix pair $(\mathbf{Q}_v^{(t)}, \mathbf{W}^H\mathbf{W})$ and the optimal solution is given by the dominant generalized eigenvector of this matrix pair. Namely, the beamformer can be optimized as

$$\mathbf{v}^{(t+1)} = \sqrt{P_{\text{av}}} \cdot \frac{\boldsymbol{\mu}_{\max}^{(t)}}{\|\mathbf{W}\boldsymbol{\mu}_{\max}^{(t)}\|}, \tag{12}$$

which is aligned with the dominant eigenvector solution and scaled to meet the total power constraint with equality.

B. Holographic Beamforming

Note that based on the considered holographic architecture, we can decompose the holographic beamformer into two parts as $\mathbf{W} = \text{diag}([w_1, w_2, \ldots, w_M])\boldsymbol{\Phi}$, where the diagonal elements w_m represent the adjustable weight of the holographic beamformer, and $\boldsymbol{\Phi}$ contains fixed phase components, which are determined by the reference wave propagating within the waveguide. Let $\mathbf{C}_b, \mathbf{D}_b, \mathbf{C}_e, \mathbf{D}_e$ be defined as

$$\begin{aligned}
\mathbf{C}_b &= \text{diag}(\boldsymbol{\Phi}\mathbf{v})^H \mathbf{h}_b\mathbf{h}_b^H \,\text{diag}(\boldsymbol{\Phi}\mathbf{v}),\\
\mathbf{D}_b &= \text{diag}(\boldsymbol{\Phi}\mathbf{z})^H \mathbf{h}_b\mathbf{h}_b^H \,\text{diag}(\boldsymbol{\Phi}\mathbf{z}),\\
\mathbf{C}_e &= \text{diag}(\boldsymbol{\Phi}\mathbf{v})^H \mathbf{g}_e\mathbf{g}_e^H \,\text{diag}(\boldsymbol{\Phi}\mathbf{v}),\\
\mathbf{D}_e &= \text{diag}(\boldsymbol{\Phi}\mathbf{z})^H \mathbf{g}_e\mathbf{g}_e^H \,\text{diag}(\boldsymbol{\Phi}\mathbf{z}).
\end{aligned} \tag{13}$$

By using the properties of the diag$(\cdot)$ operator, we can restate the problem (14) as

$$\max_{\mathbf{w}} \left[\log_2\left(1+\frac{\mathbf{w}^T\mathbf{C}_b\mathbf{w}}{\mathbf{w}^T\mathbf{D}_b\mathbf{w}+\sigma_a^2}\right) - \log_2\left(1+\frac{\mathbf{w}^T\mathbf{C}_e\mathbf{w}}{\mathbf{w}^T\mathbf{D}_e\mathbf{w}+\sigma_b^2}\right)\right]^+ \tag{14a}$$

$$\text{s.t.} \quad 0 \leq w_m \leq 1, \quad \forall m \in \{1, \ldots, M\}. \tag{14b}$$

Note that by using the properties of the logarithm function, we can rewrite it as

$$\begin{aligned}
R_s(\mathbf{w}) = \Big[&\log_2\left(\mathbf{w}^T(\mathbf{C}_b+\mathbf{D}_b)\mathbf{w}+\sigma_a^2\right) - \log_2\left(\mathbf{w}^T\mathbf{D}_b\mathbf{w}+\sigma_a^2\right)\\
&- \log_2\left(\mathbf{w}^T(\mathbf{C}_e+\mathbf{D}_e)\mathbf{w}+\sigma_b^2\right)\\
&+ \log_2\left(\mathbf{w}^T\mathbf{D}_e\mathbf{w}+\sigma_b^2\right)\Big]^+.
\end{aligned} \tag{15}$$

It minorizer can be constructed as follows. For any point $\mathbf{w} \in \mathbb{R}^M$, the following function

$$\begin{aligned}
\mathcal{L}_w^{(k)}(\mathbf{w}) = \Big[&\log_2\left(\mathbf{w}^T(\mathbf{C}_b+\mathbf{D}_b)\mathbf{w}+\sigma_a^2\right)\\
&+ \log_2\left(\mathbf{w}^T\mathbf{D}_e\mathbf{w}+\sigma_b^2\right)\\
&- \nabla f_2(\mathbf{w}^{(k)})^T\mathbf{w} - \nabla f_3(\mathbf{w}^{(k)})^T\mathbf{w} + \text{const}\Big]^+
\end{aligned} \tag{16}$$

is a valid minorizer of $R_s(\mathbf{w})$ at $\mathbf{w}^{(k)}$, where

$$\nabla f_2(\mathbf{w}) = \frac{2}{\ln 2} \cdot \frac{\mathbf{D}_b\mathbf{w}}{\mathbf{w}^T\mathbf{D}_b\mathbf{w}+\sigma_a^2}, \tag{17}$$

$$\nabla f_3(\mathbf{w}) = \frac{2}{\ln 2} \cdot \frac{(\mathbf{C}_e+\mathbf{D}_e)\mathbf{w}}{\mathbf{w}^T(\mathbf{C}_e+\mathbf{D}_e)\mathbf{w}+\sigma_b^2}. \tag{18}$$

Given the surrogate, the optimization problem with respect to the holographic beamformer at iteration k can be restated as

$$\max_{\mathbf{w}} \quad \mathcal{L}_w^{(k)}(\mathbf{w}) \tag{19a}$$

$$\text{s.t.} \quad 0 \leq w_m \leq 1, \quad \forall m \in \{1, \ldots, M\}. \tag{19b}$$

To maximize the concave surrogate function obtained in the minorization step, we employ a projected gradient ascent (PGA) algorithm. This approach leverages the smoothness and concavity of the surrogate objective while handling the box constraints in a simple yet effective manner.

Given the concave minorizer at iteration k, we define the smooth objective function $\phi(\mathbf{w})$, ignoring the outer $[\cdot]^+$ operator during optimization and also the box constraint, as (19b)

$$\phi(\mathbf{w}) = \log_2\left(\mathbf{w}^T\mathbf{A}_1\mathbf{w}+\sigma_a^2\right) + \log_2\left(\mathbf{w}^T\mathbf{A}_2\mathbf{w}+\sigma_b^2\right) - \mathbf{c}^T\mathbf{w}, \tag{20}$$

where the variables $\mathbf{A}_1, \mathbf{A}_2$ and $\mathbf{c}$ are defined as

$$\mathbf{A}_1 = \mathbf{C}_b + \mathbf{D}_b, \quad \mathbf{A}_2 = \mathbf{D}_e, \quad \mathbf{c} = \nabla f_2(\mathbf{w}^{(k)}) + \nabla f_3(\mathbf{w}^{(k)}). \tag{21}$$

Remark that the function $\phi(\mathbf{w})$ is differentiable and concave. Its gradient can be computed as

$$\nabla\phi(\mathbf{w}) = \frac{2}{\ln 2}\left(\frac{\mathbf{A}_1\mathbf{w}}{\mathbf{w}^T\mathbf{A}_1\mathbf{w}+\sigma_a^2} + \frac{\mathbf{A}_2\mathbf{w}}{\mathbf{w}^T\mathbf{A}_2\mathbf{w}+\sigma_b^2}\right) - \mathbf{c}. \tag{22}$$

Let η denote the step size at each iteration. The holographic beamformer can be optimized iteratively until convergence with the following update rule

$$\mathbf{w}^{(k+1)} = \left(\mathbf{w}^{(k)} + \eta^{(k)}\nabla\phi(\mathbf{w}^{(k)})\right). \tag{23}$$

However, the optimization is subject to box constraints, namely, that each component w_m of $\mathbf{w}$ must lie within the interval $[0, 1]$. To ensure feasibility after the gradient step, a projection operation is applied. This projection maps each entry $w_m^{(t+1)}$ back into the feasible set. Formally, the projected update $\forall m$ is given by

$$w_m^{(k+1)} = \begin{cases} 0, & \text{if } w_m^{(k+1)} < 0,\\ 1, & \text{if } w_m^{(k+1)} > 1,\\ w_m^{(k+1)}, & \text{otherwise.} \end{cases} \tag{24}$$

This projection operation can equivalently be expressed more compactly by using min and max functions as

$$w_m^{(k+1)} = \min\left(1, \max\left(0, w_m^{(k+1)}\right)\right). \tag{25}$$

This process guarantees that after each iteration, the updated holographic beamformer $\mathbf{w}^{(k+1)}$ remains feasible with respect to the amplitude constraints of the system, thus preserving the validity of the subsequent optimization steps. The effective

Algorithm 1 MM-Based Secrecy Rate Maximization

Input: $\mathbf{v}^{(0)}, \mathbf{w}^{(0)}, P_t, \eta, T_{\max}, \epsilon$.
Initialize: $t = 0$.
repeat
    Step 1: Digital BF Update
    1) Solve $\mathbf{Q}_v^{(t)}\mathbf{v} = \lambda(\mathbf{W}^H\mathbf{W})\mathbf{v}$ for largest eigenvalue λ.
    2) Update $\mathbf{v}$ as in (12).
    Step 2: Holographic BF Update
    1) Construct the minorizer as (16).
    2) Update $\mathbf{w}$ as in (25).
    $t \leftarrow t + 1$.
until The objective function converges or $t \geq T_{\max}$
Output: $\mathbf{v}$ and $\mathbf{W}$.

secrecy rate is then computed by incorporating again the function $[\cdot]^+$. The algorithmic steps to optimize the holographic beamformer are formally stated in Algorithm 1.

Convergence Analysis: The convergence of the proposed optimization algorithm is ensured by the MM framework and gradient ascent-based updates. The MM method constructs a surrogate function that upper-bounds the original non-convex objective while preserving its value at the current iteration, ensuring monotonic improvement:

$$f(\mathbf{x}^{(t+1)}) \geq f(\mathbf{x}^{(t)}). \tag{26}$$

For digital beamforming, the generalized eigenvalue solution provides an optimal unconstrained update, followed by power scaling to enforce feasibility. The holographic beamformer is optimized using gradient ascent:

$$\mathbf{x}^{(t+1)} = \mathbf{x}^{(t)} + \eta \nabla_{\mathbf{x}} g(\mathbf{x} \mid \mathbf{x}^{(t)}), \tag{27}$$

where $\eta > 0$ is the step size, and projection onto the feasible set ensures amplitude constraints are met. Since the secrecy rate is upper-bounded by the finite power budget P_t and increases monotonically, the algorithm converges to a stationary point, guaranteeing locally optimal performance.

Complexity Analysis: The complexity of the proposed design is $\mathcal{O}(T \cdot (R^3 + T_h M^2))$, where T is the number of outer iterations, T_h is the number of gradient ascent iterations for holographic beamforming, R is the number of RF chains and M is the number of RHS elements.

IV. Simulation Results

In this section, we present simulation results to evaluate the performance of the proposed algorithm for secrecy rate maximization in RHS-assisted secure holographic communications.

The noise power at Bob and Eve is fixed at -75 dBm, and the results are evaluated for varying transmit power levels. The carrier frequency is set to 30 GHz, and the element spacing on the RHS is assumed to be $\lambda/3$. The holographic beamformer employs iterative amplitude optimization with a convergence threshold of $\epsilon = 10^{-5}$ and a learning rate of $\eta = 0.01$. Given the free-space propagation vector $\mathbf{k}_f$ and the RHS propagation vector $\mathbf{k}_s$, the relationship between them is governed by the relative permittivity of the RHS substrate, ϵ_r, typically valued

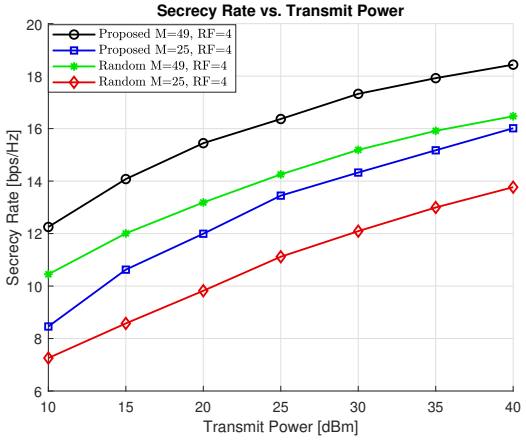

Fig. 2: Secrecy rate as a function of the transmit power with varying RHS sizes and 4 RF chains.

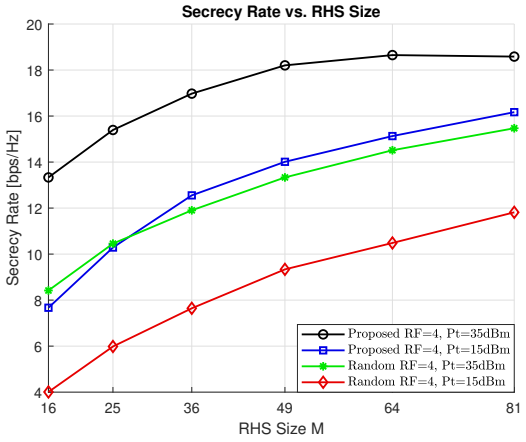

Fig. 3: Secrecy rate as a function of the RHS size with varying transmit power and 4 RF chains.

at 3, such that $|\mathbf{k}_s| = \sqrt{\epsilon_r}|\mathbf{k}_f|$. For this system, we adopt standard values commonly used in the literature: $|\mathbf{k}_f| = 200\pi$ and $|\mathbf{k}_s| = 200\sqrt{3}\pi$, as discussed in [16]. The RHS is assumed to be placed at the altitude of 50 meters, with the surface aligned in the (x, y)-plane. Bob's position is fixed directly in front of the RHS at a distance of 100 meters, while Eve's position is randomly distributed within a circle of radius 5 meters centered around Bob. We model the channels as Rician fading with the Rician factor 1. The LoS component for Bob and Eve is modelled with path loss exponents $\beta_b = 2.2$ and $\beta_e = 2.5$, respectively. The RHS response is modelled as uniform planner arrays. The number of RF chains is set to 4, and the reported results are averaged over 100 channel realizations.

Figure 2 illustrates the secrecy rate as a function of the transmit power in dBm, with the number of RF chains set to $R = 4$. It is clearly visible that the proposed method consistently outperforms the benchmark scheme across all power levels for both RHS sizes. The secrecy rate improvement is particularly significant at lower power levels, demonstrating the effectiveness of the optimized beamforming in efficiently

utilizing available power. In contrast, the benchmark method exhibits a much slower secrecy rate increase and saturates earlier, indicating its limited capability in mitigating interference and enhancing security. This highlights the advantage of the proposed approach in dynamically adapting the holographic beamforming strategy to maximize secrecy performance under varying power conditions.

Figure 3 illustrates the secrecy rate performance as a function of the RHS size M, with the number of RF chains set to $R = 4$. As observed, the proposed method consistently achieves a significantly higher secrecy rate across all values of M, demonstrating its enhanced beamforming capabilities compared to the benchmark scheme. This improvement stems from the ability of the optimized beamforming approach to better exploit the increased spatial degrees of freedom provided by the RHS. Additionally, the superiority of the proposed method remains evident across different transmit power levels, confirming its robustness in adapting to varying power conditions with any RHS size.

From the results presented above, it is evident that the proposed method significantly enhances secrecy rate performance across different power levels and RHS sizes. The optimized beamforming strategy demonstrates superior efficiency, particularly at lower power levels, where it effectively utilizes available power to mitigate interference and improve security. In contrast, the benchmark scheme shows a much slower secrecy rate increase and saturates earlier, highlighting its limitations in adapting to varying power conditions. Additionally, the proposed approach consistently outperforms the benchmark across all RHS sizes, showcasing its ability to fully exploit the increased spatial degrees of freedom provided by a larger RHS.

V. Conclusion

This paper proposed a novel optimization framework for maximizing the secrecy rate in RHS-assisted systems by jointly optimizing digital and analog holographic beamforming. Leveraging a MM-based approach, the method effectively tackled the inherent non-convexity of the problem, ensuring reliable convergence to locally optimal solutions. Simulation results demonstrated substantial secrecy rate improvements over the benchmark scheme. The proposed approach also exhibited robustness across varying power levels and RHS sizes, maintaining superior performance under different system conditions. Additionally, the results confirmed that increasing the RHS size leads to a monotonic improvement in secrecy rate, as the additional reconfigurable elements enable finer beam control and better interference mitigation

References

[1] W. U. Khan, A. Mahmood, C. K. Sheemar, E. Lagunas, S. Chatzinotas, and B. Ottersten, "Reconfigurable intelligent surfaces for 6G non-terrestrial networks: Assisting connectivity from the sky," *IEEE Internet of Things Magazine*, vol. 7, no. 1, pp. 34–39, 2024.

[2] G. Iacovelli, C. K. Sheemar, W. U. Khan, A. Mahmood, G. C. Alexandropoulos, J. Querol, and S. Chatzinotas, "Holographic MIMO for next generation non-terrestrial networks: Motivation, opportunities, and challenges," *arXiv preprint arXiv:2411.10014*, 2024.

[3] S. Bahanshal, Q.-U.-A. Nadeem, and M. Jahangir Hossain, "Holographic MIMO: How many antennas do we need for energy efficient communication?" *IEEE Trans. Wirel. Commun.*, vol. 24, no. 1, pp. 118–133, 2025.

[4] C. K. Sheemar, W. U. Khan, G. C. Alexandropoulos, M. Ahmed, and S. Chatzinotas, "Minimum mean squared error holographic beamforming for sum-rate maximization," *arXiv preprint arXiv:2503.17205*, 2025.

[5] J. C. Ruiz-Sicilia, M. Di Renzo, M. D. Migliore, M. Debbah, and H. V. Poor, "On the degrees of freedom and eigenfunctions of line-of-sight holographic MIMO communications," *arXiv preprint arXiv:2308.08009*, 2023.

[6] J. C. Ruiz-Sicilia, M. Di Renzo, M. Debbah, and H. V. Poor, "Low complexity optimization for line-of-sight RIS-aided holographic communications," in *IEEE 31st European Signal Processing Conference (EUSIPCO)*, 2023, pp. 900–904.

[7] C. K. Sheemar, W. U. Khan, G. Alexandropoulos, J. Querol, and S. Chatzinotas, "Holographic joint communications and sensing with Cramer-Rao bounds," *arXiv preprint arXiv:2502.15248*, 2025.

[8] C. K. Sheemar, A. Mahmood, C. K. Thomas, G. C. Alexandropoulos, J. Querol, S. Chatzinotas, and W. Saad, "Joint beamforming and 3D location optimization for multi-user holographic UAV communications," *arXiv preprint arXiv:2502.17428*, 2025.

[9] C. K. Sheemar, C. K. Thomas, G. C. Alexandropoulos, J. Querol, S. Chatzinotas, and W. Saad, "Joint holographic beamforming and user scheduling with individual QoS constraints," *IEEE Transactions on Vehicular Technology*, pp. 1–15, 2025.

[10] A. S. de Sena, J. He, A. Al Hammadi, C. Huang, F. Bader, M. Debbah, and M. Fink, "On the sum secrecy rate of multi-user holographic MIMO networks," in *IEEE ICC*, 2024, pp. 4390–4396.

[11] Y. Xu, J. Liu, X. Wu, T. Guo, and H. Peng, "Reconfigurable holographic surface-assisted wireless secrecy communication system," *Electronics*, vol. 13, no. 7, p. 1359, 2024.

[12] R. Deng, B. Di, H. Zhang, Y. Tan, and L. Song, "Reconfigurable holographic surface: Holographic beamforming for metasurface-aided wireless communications," *IEEE Transactions on Vehicular Technology*, vol. 70, no. 6, pp. 6255–6259, 2021.

[13] Y. Sun, P. Babu, and D. P. Palomar, "Majorization-minimization algorithms in signal processing, communications, and machine learning," *IEEE Transactions on Signal Processing*, vol. 65, no. 3, pp. 794–816, 2017.

[14] C. K. Sheemar, S. Chatzinotas, D. Slock, E. Lagunas, and J. Querol, "Parallel and distributed hybrid beamforming for multicell millimeter wave MIMO full duplex," *IEEE Transactions on Vehicular Technology*, vol. 74, no. 3, pp. 4289–4306, 2025.

[15] S.-J. Kim and G. B. Giannakis, "Optimal resource allocation for MIMO ad hoc cognitive radio networks," *IEEE Transactions on Information Theory*, vol. 57, no. 5, pp. 3117–3131, 2011.

[16] R. Deng, B. Di, H. Zhang, Y. Tan, and L. Song, "Reconfigurable holographic surface-enabled multi-user wireless communications: Amplitude-controlled holographic beamforming," *IEEE Trans. Wirel. Commun.*, vol. 21, no. 8, pp. 6003–6017, 2022.